Journal of Modern Materials
ISSN: 2456-4834
Volume 3, Issue 1, pp. 33-40, 2017
DOI: https://doi.org/10.21467/jmm.3.1.33-40

RESEARCH ARTICLE

Calculation of Normalized Pinning Force and Nature of Pinning Mechanism for Nano-Al Doped MgB_2 Superconductor

Intikhab A. Ansari

Department of General Studies, Jubail Industrial College, P. O. Box - 10099,
Jubail Industrial City-31961, Saudi Arabia.

* Corresponding author email: intikhabansari@yahoo.com

Received: 31 January 2017 / Accepted: 2 February 2017 / Published: 3 February 2017

ABSTRACT

The $J_c(H)$ of nano-Al doped MgB_2 samples has been calculated from $M(H)$ loop measurements at different temperatures. Normalized volume pinning forces as a function of the reduced field have been analyzed at different temperatures and doping level which was taken from the $J_c(H)$ data. The modified scaling law was used as discussed by the Eisterer to analyze the pinning forces. This law was compared with the scaling law used by the Fietz and co-worker. The grain boundary pinning is found the dominant pinning mechanism in all the doped samples and exhibit the scaling behavior. The XRD and temperature dependence of resistivity confirms the successful substitution of nano-Al at Mg sites. The results endorse that the magnetic anisotropy decreased from pure to the dirty limit with the doping of the nano-Al. The enhancement in the $J_c(H)$ of the sample with the nano-Al doping is due to decrease in the anisotropy and increase in the volume pinning forces. The 2 % nano-Al doped sample between 15–30 K shows the highest $J_c(H)$ among all the samples.

Keywords: Pinning force density; Critical current; MgB_2; Nano-Al doping

1. Introduction

In the last decades, the MgB_2 demonstrates itself as a promising candidate for the practical applications due to its simple crystal structure, large coherence length, relatively high-temperature (T_c) and economical cost. However, the high critical current (J_c) of the bulk materials in magnetic field plays an important role in high field industrial applications [1]. The existence of high J_c up to 10^6 A/cm^2 has been reported in the lots of literature. The value of J_c in pure material abruptly decreases in the presence of a high magnetic field. The effective improvement in J_c has been noticed due to the increase of pinning centers served by grain boundaries. Enormous efforts have been accustomed in order to enhance the J_c under the magnetic field [2]–[8]. The nanoparticle doping is one of the methods to improve the poor grain connection in pure MgB_2. Introducing more pinning centers in the pristine MgB_2 sample, exclusively nano size inclusions, generally provides a strong pinning force. The magnitude of bulk pinning force density, F_p can be calculated by the critical current density and an applied field, $J_c \times H$. The F_p was recently used to analyze the nature of pinning behavior in the nano-Zn doped MgB_2 sample [9]. The F_p in the superconductor can be evaluated from the magnetization measurement at a particular temperature and is managed by the presence of impurities and microstructure of the materials. Fietz and co-worker [10] proposed the following scaling law for the normalized pinning force density $f \propto b^p(1-b)^q$, where $f = F_p(b) = F_p / F_{p,max}$ is the normalized pinning force density, $F_{p,max}$ is the maximum pinning force density, $b = H / H_{irr}$ is the reduced field and H_{irr} is the irreversibility field where J_c practically becomes zero. The function $F_p(b)$ shows a

maximum value at $b_{peak} = p/(p+q)$. The exponents p and q are the characteristic for the prevailing pinning mechanism. Instantly, p is predicted to be 1/2 for grain boundary pinning or 1 for normal point pinning, while q is same in both cases in this report. The study of the normalized volume pinning force as a function of field gives us the chance to know the behavior of the pinning mechanism in an individual case [11]. However, the MgB_2 retains an intrinsic anisotropy in the presence of magnetic field [12], [13], the super-currents never flow consistently because of the grain disorientation distribution on a sample surface. The clean grain boundaries not only drift the current in MgB_2 [1] but also behave as effective pinning centers [14] and permit high currents in un-textured polycrystalline samples. Furthermore, secondary phases partly obstruct the current flow over the surface of the grains [15] and diminish the actual area over which the super-currents flow [16]. This problem is elaborated by the voids and secondary phases present over the surface of the grains that turn to inflate the current percolation, which is a usually inevitable result of the magnetic anisotropy [17].

The present study described the detailed analysis of the J_c and normalized pinning force, f as a function of magnetic field and temperature for nano Al doped MgB_2 sample using the simple scaling law described above. The difference between the previous report [6] and present is that in the prior report only magnetic behavior have been analyzed but in the present report I have calculated the J_c as well as the pinning mechanism for nano Al doped MgB_2. In order to examine the dominant pinning mechanism for nano Al doped MgB_2 sample this scaling law describes the significant results. In addition, it is shown that peak in reduced field dependence of the normalized pinning force is extensively shifted to the lower field by the anisotropy. The nano-Al doping may also affect the grain growth, thus leading to an improvement in the J_c.

2. Experimental Details

$Mg_{1-x}Al_xB_2$ with different doping levels (x = 0, 2, 4, and 6 at. %) were synthesized by *in-situ* standard solid state reaction method under high vacuum as described elsewhere in detail [6]. The starting material powders (purity > 99%) were mixed in the stoichiometric ratio supplied by Sigma-Aldrich. Here, the source of the nano-Al powder was nano-Al_2O_3. Finally, the bulk polycrystalline samples of the nano-Al doped MgB_2 were achieved. The phase components were identified by the powder X-ray diffraction (XRD) measurement using Cu K_α radiation. The lattice parameters were calculated from the peak positions of the XRD plots. The transition temperature, T_c of the samples was determined by the temperature dependence of resistivity measurement using four-probe technique. The critical current density, J_c values were deduced from the hysteresis loop $M(H)$ using Bean's model. The DC magnetizations of these samples were measured using a PAR-4500 Vibrating Sample Magnetometer (VSM).

3. Results and Discussion

The x-ray diffraction (XRD) pattern of the doped and undoped MgB_2 samples with different nano Al-concentration (0%, 2%, 4% and 6%) is shown in Figure 1.

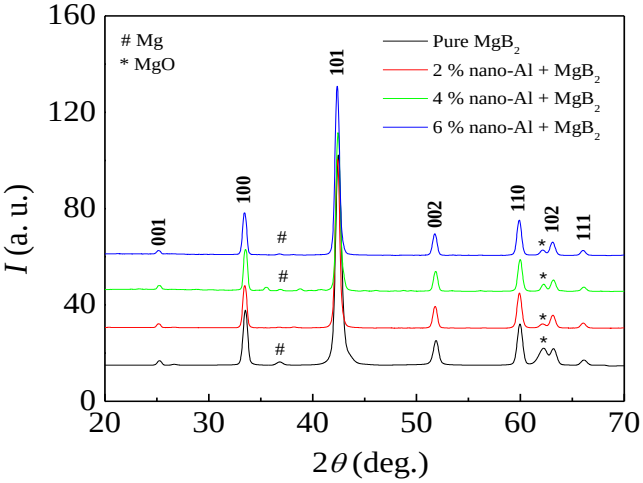

Figure 1: *XRD pattern of 0%, 2%, 4% and 6% nano-Al doped MgB_2 (Color figure online)*

All the sample shows the MgB_2 as the dominant phase with minor impurity of MgO and un-reacted Mg. The Figure 1 of the present study indicates that MgO phase gradually decreased with the increasing doping level except the 6% sample. Thus, it concludes that the oxygen which comes from dopant is effectively removed during a powder mixing process. The value of a lattice parameter as well as c lattice parameter decreased with the increase of the nano Al doping

concentration. The *a* lattice parameter decreased from 3.087–3.081 Å on the other hand the *c* lattice parameter suppressed from 3.524–3.350 Å. It is evident from these results that nano Al atoms partially occupied the sites of Mg in the MgB_2 matrix. It is furthermore necessary to study the effect of nano Al dopant on the temperature dependence of resistivity which is described in the Figure 2.

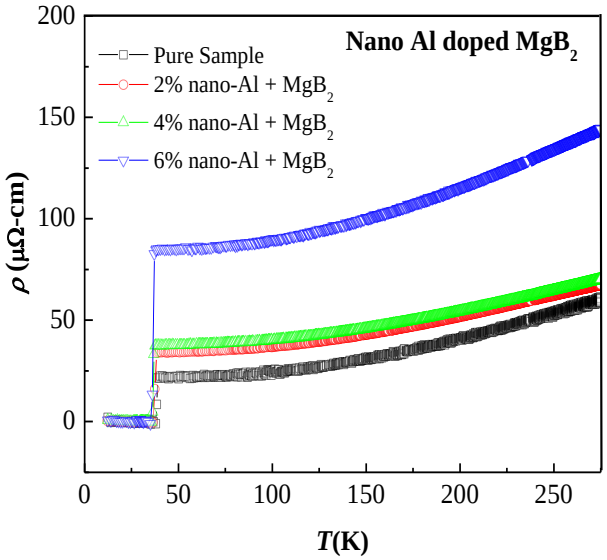

Figure 2: *Temperature dependence of the resistivity of the nano-Al doped MgB_2 samples.*

It is remarkable that the normal-state resistivities of all the samples are almost the same except the 6% doped sample. The later might be distinct due to the formation of dominant impurity phase MgO at grain boundaries in this doped sample. The residual resistivity ratio (RRR) values shows the reduction from 3–1.82 with the increase of doping level. The temperature dependence of electrical resistivity of all the samples helps in order to understand the electron-phonon interaction, which is described by the Bloch-Gruneisen integral [18]. The nano-Al substitution is further supported from the change in the T_c of the doped samples as shown in the Table 1.

Table 1: *Variation of a-lattice parameter, c-lattice parameter and transition temperature T_c with the nano-Al doped MgB_2*

x(%)	*a*(Å)	*c*(Å)	T_c(K)
0.0	3.087	3.524	38
2.0	3.085	3.522	36
4.0	3.083	3.351	36
6.0	3.081	3.350	35

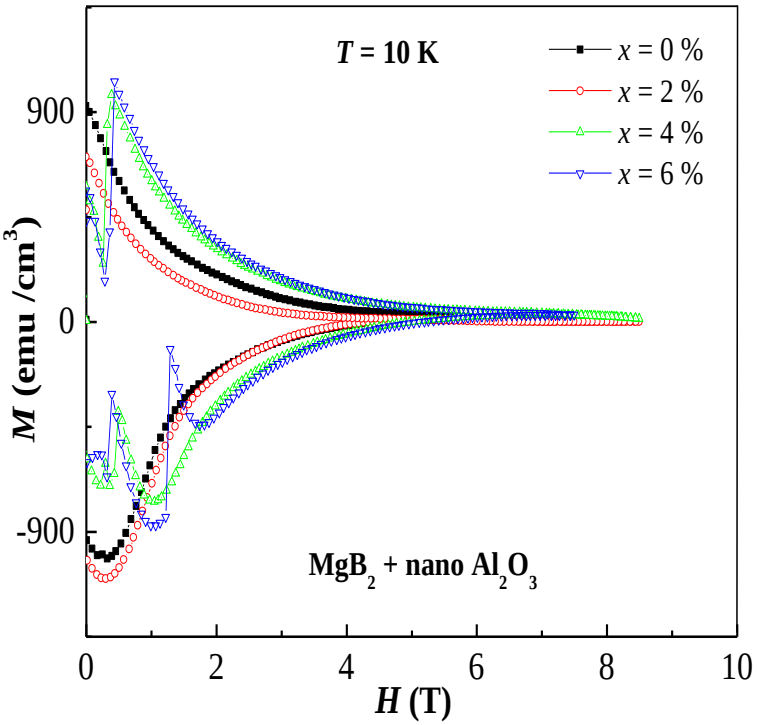

Figure 3: *Hysteresis loops of all the samples at 10 K. Avalanches are observed at low doping levels (Color figure online)*

Figure 3 shows the hysteresis loops of all the samples at 10 K with a DC field. It is clear that the pure sample shows continuous hysteresis loop while the doped samples show sharp flux jumps below 2T. As shown in Figure 3 at 10K, the 6% sample exhibit the better *M*(H) behavior among all the samples. Zhao *et al.* [19] described that using a SQUID for magnetization measurements, avalanches vanish due to the very low speed of data acquisition. In order to further find out evidences, the magnetic field dependence of J_c at different temperature has been calculated under different doping level.

Figure 4 shows the magnetic field dependence of J_c at 10, 15, 20 and 30K for pure and nano Al-doped MgB_2 samples. It is evident from the figure that the value of J_c is gradually improved of 2% doped sample in the temperature range from 15–30K. At 10K temperature, the 6% sample exhibit the better J_c(H) behavior among all the four samples. Furthermore, at 15K temperature, all the doped sample shows relatively same J_c value at lower field but when the field enhances the difference in J_c becomes comparatively enough as the prior. The 2% nano-Al doped sample offered the highest J_c at 15–30 K but not at 10 K because

at lower temperatures (< 15 K), there might be some kind of cross-over taken place in the 2% sample. On the contrary, the pinning strength is a function of the temperature. For 2% sample, at lower temperature (< 15 K), the pinning is higher and at higher temperature (> 15 K) the pinning strength becomes weak and actual grain connectivity plays the role of carrying the current. This explains the cross-over of J_c plot around 15 K for 2% nano-Al doped sample. Due to the flux avalanches (instabilities) in $M(H)$ plot (some of them are reported elsewhere [6]), there are some jumps reflected at 10K (nearby 1T) and 20K (nearby 3.5T) for 6% doped and pure sample, respectively as shown in the Figure 4. In addition, at 30K temperature the 4% and 6% Al doped sample depicts some jumps as well close to 0.25T field. There are two kinds of avalanches in superconductors, as pointed out by Altshuler and Johansen [20]. The first one refers to the dynamical driven avalanches, i.e., small isothermal avalanches related to the evolution of the critical state model. The second type refers to thermally driven avalanches, also called flux avalanches, and they are related to thermomagnetic instabilities, leading to a sudden penetration of flux in an approximately adiabatic process, as discussed by Mints and Rakhmanov [21]. One of the signatures of the flux avalanches is a jumpy behavior in $M(H)$ curves, which named these phenomena as flux jumps. In order to further find out evidences, the normalized pinning force has been calculated as a function of reduced field under different doping level and temperature. It is remarkable that the critical field J_c is directly proportional to the $F_{p,max}$.

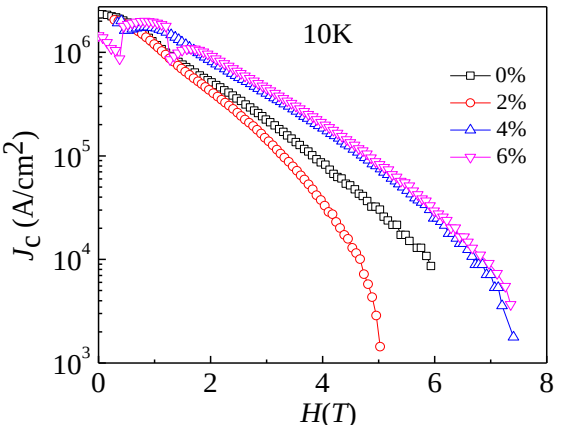

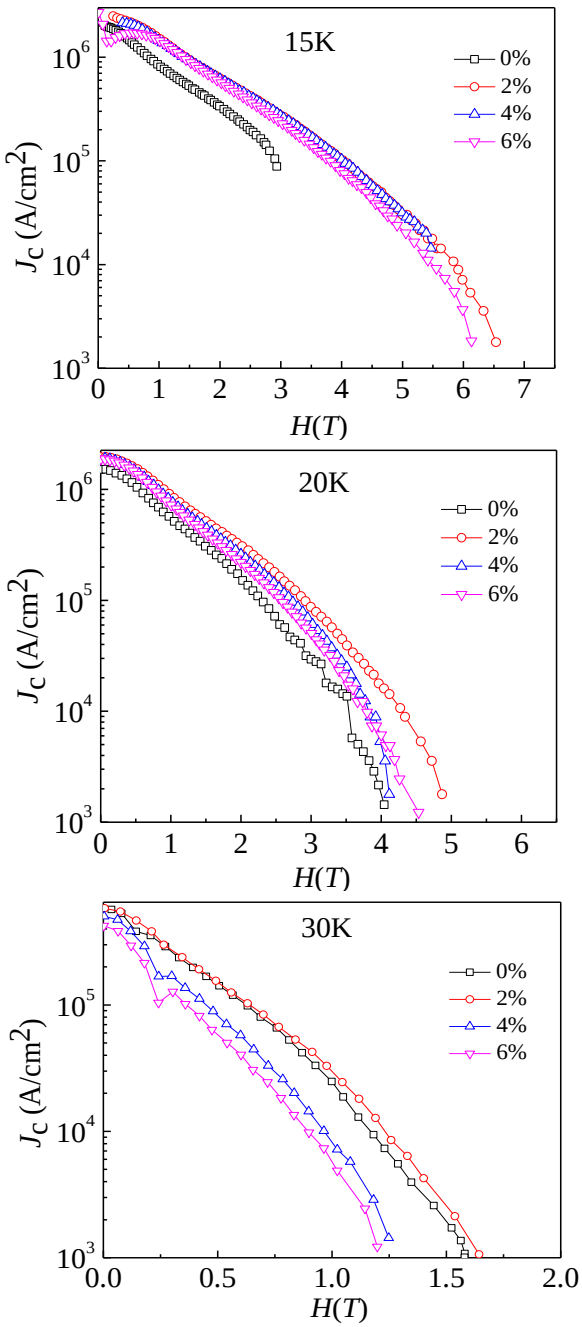

Figure 4: *Magnetic field dependence of J_c at difference temperatures for $Mg_{1-x}Al_xB_2$ (Color figure online)*

In order to study the characteristics of the pinning mechanism for different Al doped MgB_2 samples, the normalized volume pinning force (F_p / $F_{p,\,max}$) as a function of reduced field (H/ H_{irr}) has been analyzed at different temperatures. The left column of the Figure 5 has shown the outcomes of these samples.

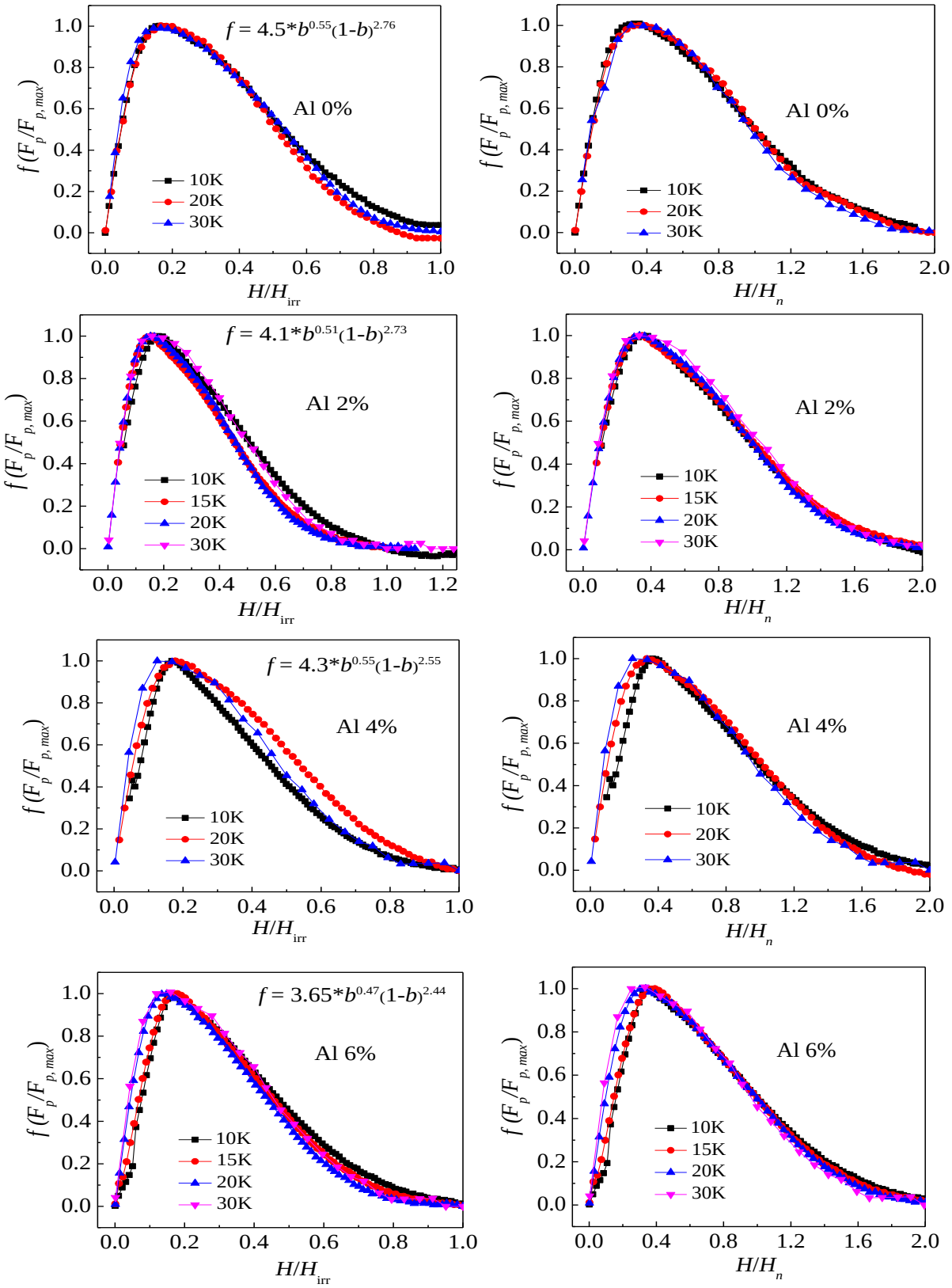

Figure 5*: Normalized pinning force as a function of (left column) reduced field (H/H_{irr}) and (right column) modified reduced field (H/H_n). (Color figure online)*

Table 2: *The value of b_{peak} and b_{npeak} for all samples at different temperature*

***T*(K)/ *x* %**	**0%**		**2%**		**4%**		**6%**	
	b_{peak}	b_{npeak}	b_{peak}	b_{npeak}	b_{peak}	b_{npeak}	b_{peak}	b_{npeak}
10	0.151	0.285	0.161	0.341	0.167	0.353	0.181	0.366
15	-	0.348	0.157	0.349	-	0.358	0.179	0.391
20	0.149	0.326	0.152	0.332	0.166	0.333	0.177	0.336
30	0.119	0.249	0.121	0.250	0.124	0.312	0.157	0.328

It is evident from the Figure 5 that the dominant pinning occurs in undoped, 2% and 6% nano Al doped samples at different temperatures and follow the scaling law $f \propto b^p(1-b)^q$. In case of undoped sample the values of p and q are observed to be 0.55 and 2.75, respectively which is in agreement with the value of p and q for grain boundary pinning ($p = 1/2$ and $q = 2$). In case of 2% and 6% Al doped samples the values of p are 0.51 and 0.47 while the values of q are 2.73 and 2.44, respectively. These values are still approaching to the grain boundary pinning. The 4% sample shows the different behavior at different temperatures and does not coincide at all. The values of the p and q are still close to the grain boundary pinning in case of 4% sample but the disperse might be due to the fluctuation in the $M(H)$ plot at lower J_c value.

To understand the in-depth effect of the nano-Al doped MgB_2 on the nature of pinning, the peak position in f ($F_p / F_{p,\,max}$) vs. H/H_{irr} plot has been taken into account which is indicated by b_{peak} here. In the isotropic materials, the F_{max} occurs at $b_{peak} = 0.2$ for grain boundary pinning and $b_{peak} = 0.33$ for point pinning. The shift of b_{peak} of the normalized volume pinning force depends not only on the dominant pinning mechanism but also on the anisotropy γ and on the percolation threshold p_c. The effect of the anisotropy on scaling which generally gives the deviation of the peak position in the different pinning mechanism has been studied theoretically for pure MgB_2 system as proposed by the Eisterer [22]. He reported that the significant anisotropic changes occurs due to the field dependence of the volume pinning force in the polycrystalline samples. In the pure MgB_2, the value of p_c varies minutely (0.25 to 0.30) but the value of γ alters between 1 (dirty limit) to 6 (clean limit). The maximum peak field value (b_{peak}) is hyper-sensitive to the anisotropy γ rather than percolation threshold p_c. Therefore, analyzing the pinning behavior from the b_{peak} only without prior knowledge of γ and p_c is challenging using the scaling law where $b = H / H_{irr}$ is involved. To reduce this difficulty, Eisterer has proposed the modified scaling law to study the pinning mechanism in bulk samples in which anisotropy γ and percolation threshold p_c has minor effect on peak field position. In this new law f is plotted as a function of normalized field $b_{npeak} = H / H_n$ where H_n is the field at which the pinning force becomes half of $F_{p,\,max}$ value. He theoretically explained that the peak position shifts very slightly, 3% only in case of grain boundary pinning ($b_{npeak} = 0.341$ to 0.352) and 6% in case of the point pinning ($b_{npeak} = 0.465$ to 0.491) from clean to dirty sample respectively in both conditions. It is easily possible to distinguish between grain boundary pinning and point pinning from just the difference of peak field position (0.341 to 0.465), which differ by nearly 36%. The new scaling scheme for nano-Al doped MgB_2 sample is mentioned in the right column of Figure 5, which articulates the better overlapping of the data acquisition for different temperatures. The values of b_{peak} and b_{npeak} which shows the peak position in H/H_{irr} and H/H_n plot, respectively are exposed in Table 2 for different samples at different temperatures. Eisterer has revealed that b_{peak} or b_{npeak} shift towards lower field value as the anisotropy enhances. Due to large flux avalanche (instability) in $M(H)$ plot at 15K in pure and 4% doped sample, the data is absent at 15K in f vs. reduced field plot for these samples. From Figure 5 and Table 2 as well, it is evident that the grain boundary pinning is the dominant pinning mechanism in all the four samples at different

temperature. Table 2 clearly shows the enhancement of b_{peak} value in the Al-doped samples in comparison with pure sample. This represents that nano Al_2O_3 has decreased the magnetic anisotropy from pure to dirty limit. It is notable that as the Al doping increases the sample becomes less anisotropic, on the contrary the pure sample is highly anisotropic in nature.

4. Conclusion

With the help of hysteresis loop, the $J_c(H)$ was calculated for all the doped and undoped samples at different temperatures. Among all the samples the 2% doped sample reveals the highest $J_c(H)$ at all the temperatures except 10K. The normalized pinning force density as a function of reduced field was calculated by two scaling ways as discussed by the Fietz *et al.* and Eisterer. It was confirmed that all samples show grain boundary pinning. At last, the value of b_{peak} and b_{npeak} for all samples at different temperatures has been tabulated. The increase in the value of the b_{peak} with the nano Al doping denotes that the doping decreases the anisotropy of the samples. These b_{peak} values are responsible for grain boundary pinning. Furthermore, it can be concluded that the suppression in the anisotropy is partially accountable for the enhancement of the $J_c(H)$ values.

Acknowledgments

I would like to thank Jafar Parakkandy (KSU, Riyadh) for experimental ends. This work is supported by the General Studies Department, Jubail Industrial College, Royal Commission in Jubail, Saudi Arabia under contract no. 2101349345.

How to Cite this Article:

I. Ansari, “Calculation of Normalized Pinning Force and Nature of Pinning Mechanism for Nano-Al Doped MgB_2 Superconductor”, *J. Mod. Mater.*, vol. 3, no. 1, pp. 33-40, Feb. 2017. doi: 10.21467/jmm.3.1.33-40

References

[1] D. Larbalestier, A. Gurevich, D. M. Feldmann, and A. Polyanskii, “High-Tc superconducting materials for electric power applications,” *Nature*, vol. 414, no. 6861, pp. 368–377, Nov. 2001.

[2] M. A. Susner *et al.*, “Influence of Mg/B ratio and SiC doping on microstructure and high field transport Jc in MgB2 strands,” *Phys. C Supercond.*, vol. 456, no. 1, pp. 180–187, 2007.

[3] M. Putti, M. Affronte, C. Ferdeghini, P. Manfrinetti, C. Tarantini, and E. Lehmann, “Observation of the Crossover from Two-Gap to Single-Gap Superconductivity through Specific Heat Measurements in Neutron-Irradiated MgB_2,” *Phys. Rev. Lett.*, vol. 96, no. 7, p. 77003, Feb. 2006.

[4] A. Gümbel, J. Eckert, G. Fuchs, K. Nenkov, K.-H. Müller, and L. Schultz, “Improved superconducting properties in nanocrystalline bulk MgB_2,” *Appl. Phys. Lett.*, vol. 80, no. 15, pp. 2725–2727, Apr. 2002.

[5] K. P. Singh *et al.*, “Nano Fe_3O_4 Induced Fluxoid Jumps and Low Field Enhanced Critical Current Density in MgB2 Superconductor,” *J. Supercond. Nov. Magn.*, vol. 21, no. 1, pp. 39–44, Jan. 2008.

[6] I. A. Ansari *et al.*, “The effect of nano-alumina on structural and magnetic properties of MgB_2 superconductors,” *Supercond. Sci. Technol.*, vol. 20, no. 8, pp. 827–831, Aug. 2007.

[7] S. X. Dou *et al.*, “Enhancement of the critical current density and flux pinning of MgB_2 superconductor by nanoparticle SiC doping,” *Appl. Phys. Lett.*, vol. 81, no. 18, pp. 3419–3421, Oct. 2002.

[8] H. Yamada, M. Hirakawa, H. Kumakura, A. Matsumoto, and H. Kitaguchi, “Critical current densities of powder-in-tube MgB_2 tapes fabricated with nanometer-size Mg powder,” *Appl. Phys. Lett.*, vol. 84, no. 10, pp. 1728–1730, Mar. 2004.

[9] M. Shahabuddin, I. A. Ansari, N. S. Alzayed, K. A. Ziq, and A. F. Salem, “Effect of Nano ZnO Doping on the Nature of Pinning of MgB_2 Superconductors,” *J. Supercond. Nov. Magn.*, vol. 26, no. 5, pp. 1547–1552, May 2013.

[10] W. A. Fietz and W. W. Webb, “Hysteresis in Superconducting Alloys—Temperature and Field Dependence of Dislocation Pinning in Niobium Alloys,” *Phys. Rev.*, vol. 178, no. 2, pp. 657–667, Feb. 1969.

[11] D. Dew-Hughes, “The role of grain boundaries in determining J_c in high-field high-current superconductors,” *Philos. Mag. Part B*, vol. 55, no. 4, pp. 459–479, Apr. 1987.

[12] M. Zehetmayer, M. Eisterer, J. Jun, S. M. Kazakov, J. Karpinski, and H. W. Weber, “Magnetic field dependence of the reversible mixed-state properties of superconducting MgB_2 single crystals and the influence of artificial defects,” *Phys. Rev. B*, vol. 70, no. 21, p. 214516, Dec. 2004.

[13] L. Lyard *et al.*, “Anisotropies of the Lower and Upper Critical Fields in MgB_2 Single Crystals,” *Phys. Rev. Lett.*, vol. 92, no. 5, p. 57001, Feb. 2004.

[14] E. Martínez, P. Mikheenko, M. Martínez-López, A. Millán, A. Bevan, and J. S. Abell, “Flux pinning force in bulk MgB_2 with variable grain size,” *Phys. Rev. B*, vol. 75, no. 13, p. 134515, Apr. 2007.

[15] R. F. Klie, J. C. Idrobo, N. D. Browning, K. A. Regan, N. S. Rogado, and R. J. Cava, “Direct observation of nanometer-scale Mg- and B-oxide phases at grain boundaries in MgB_2,” *Appl. Phys. Lett.*, vol. 79, no. 12, pp. 1837–1839, Sep. 2001.

[16] J. M. Rowell *et al.*, “The widely variable resistivity of MgB_2 samples,” *Supercond. Sci. Technol.*, vol. 16, no. 6, pp. R17–R27, Jun. 2003.

[17] M. Eisterer *et al.*, “Magnetic properties and critical currents of MgB_2,” *Supercond. Sci. Technol.*, vol. 20, no. 12, pp. R47–R73, Dec. 2007.

[18] I. A. Ansari, "Numerical solution of Bloch–Gruneisen function to determine the contribution of electron–phonon interaction in polycrystalline MgB_2 superconductor," *Phys. C Supercond.*, vol. 470, no. 11, pp. 508–510, 2010.

[19] Z. W. Zhao *et al.*, "Suppression of superconducting critical current density by small flux jumps in MgB_2 thin films," *Phys. Rev. B*, vol. 65, no. 6, p. 64512, Jan. 2002.

[20] E. Altshuler and T. H. Johansen, "*Colloquium* : Experiments in vortex avalanches," *Rev. Mod. Phys.*, vol. 76, no. 2, pp. 471–487, Apr. 2004.

[21] R. G. Mints and A. L. Rakhmanov, "Critical state stability in type-II superconductors and superconducting-normal-metal composites," *Rev. Mod. Phys.*, vol. 53, no. 3, pp. 551–592, Jul. 1981.

[22] M. Eisterer, "Calculation of the volume pinning force in MgB_2 superconductors," *Phys. Rev. B*, vol. 77, no. 14, p. 144524, Apr. 2008.